ISBN: 978-3-95450-208-0 doi:10.18429/JACoW-IPAC2019-TUPRB005

PHOTON POLARISATION MODELLING OF APPLE-II EPUs

M. J. Sigrist, C. K. Baribeau, T. M. Pedersen, Canadian Light Source Inc., Saskatoon, Canada

Abstract

The CLS is currently commissioning two APPLE-II insertion devices (IDs), see [1], and constructing two more that allow for operation in "universal mode", i.e. selecting arbitrary photon polarisation parameters. Two of these devices will operate in the soft x-ray range where there is expected to be a significant change to polarisation at the sample due to transmission effects of the beam line optics. Arbitrary polarisation selection of the ID will counter transmission effects and enable circular polarisation at the sample position. A polarisation model of the device is derived which allows for the calculation of both the Stokes parameters and photon energy for any set point of ID gap and phase. Numerical solutions of these equations allow the calculation of gap and phase set points for any desired photon energy or polarisation. The results of the polarisation model are compared with numerical simulations of the synchrotron radiation calculated using measured magnetic fields at various polarisation modes.

EPU GIRDER POSITIONS

Each Elliptically Polarized Undulator (EPU) allows the gap and all four sub-girders to be set independently in the range of $\pm\lambda/2$ for a magnetic period (λ). We first define two operational parameters, elliptical phase (ϕ_E) and linear phase (ϕ_L), which simplify set points for the phase girders, see [2]. The set points of the four girders can be found by summing the components from the elliptical and linear phases, $+G_1 = -G_2 = +G_3 = -G_4 = \phi_E/2$ and for $\phi_L \geq 0$ $G_1 = -G_3 = \phi_L$; $G_2 = G_4 = 0$ or $\phi_L < 0$ $G_4 = -G_2 = \phi_L$; $G_1 = G_3 = 0$. We can limit the operational phases to $|\phi_E| < \lambda/2$ and $|\phi_L| < \lambda/4$.

MAGNETIC FIELDS

The on axis vertical (z) magnetic fields of the i'th girder can be expressed as $B_{zi} = B_{z0i} \cdot \cos[k(s+G_i)]$ where B_{z0i} is the nominal field determined by the magnetic material, geometry and gap, s is the longitudinal coordinate, k is a constant equal to $2\pi/\lambda$ and G_i is the phase setting for each girder. The horizontal fields (x) have a corresponding definition. If we sum the terms for all four girders in the $\phi_L > 0$ case and substitute ϕ_E and ϕ_L for G_i values we get Eq. (1) and Eq. (2) for B_z and B_x. This description is similar to previous work for APPLE-II undulators [3] which only described purely elliptical or linear phase shifts.

$$B_z = \frac{B_{z0}}{4}\left(\begin{array}{c}\mathrm{Cos}\left[k\left(s+\frac{\phi_E}{2}+\phi_L\right)\right]+\mathrm{Cos}\left[k\left(s-\frac{\phi_E}{2}\right)\right]\\ +\mathrm{Cos}\left[k\left(s+\frac{\phi_E}{2}-\phi_L\right)\right]+\mathrm{Cos}\left[k\left(s-\frac{\phi_E}{2}\right)\right]\end{array}\right) \quad (1)$$

$$B_x = \frac{B_{x0}}{4}\left(\begin{array}{c}\mathrm{Cos}\left[k\left(s+\frac{\phi_E}{2}+\phi_L\right)\right]-\mathrm{Cos}\left[k\left(s-\frac{\phi_E}{2}\right)\right]\\ +\mathrm{Cos}\left[k\left(s+\frac{\phi_E}{2}-\phi_L\right)\right]-\mathrm{Cos}\left[k\left(s-\frac{\phi_E}{2}\right)\right]\end{array}\right) \quad (2)$$

The harmonic addition theorem can be applied to Eq. (1) and Eq. (2) to find solutions for the transverse magnetic field components. The placeholder c is used to denote either the horizontal (x) or vertical (z) field component. The fields are shown in Eq. (3) separating each magnetic field component into a nominal term (B_{c0}) dependent on gap, an amplitude term (A_c) dependent on ID phases, and the periodic cosine term with a phase shift (δ_c) dependent on ID phases.

$$B_c(g,\phi_E,\phi_L,s) = B_{c0}(g)\cdot A_c(\phi_E,\phi_L)\cdot \mathrm{Cos}\left[ks+\delta_c(\phi_E,\phi_L)\right] \quad (3)$$

The phase dependent amplitude terms and the phase shift between B_z and B_x are below. The middle sign in the amplitude is determined by the component axis, A_z +, A_x −.

$$A_z^2, A_x^2 = \frac{1}{4}\left(1\pm 2\mathrm{Cos}\left[k\phi_L\right]\mathrm{Cos}[k\phi_E]+\mathrm{Cos}^2[k\phi_L]\right)$$

$$\delta = \delta_x - \delta_z = \mathrm{Arctan}\left[\frac{-2\mathrm{Cos}\left[k\phi_L\right]\mathrm{Sin}[k\phi_E]}{\mathrm{Sin}^2[k\phi_L]}\right]$$

POLARISATION

The polarisation rates using the Stokes description can be approximated, see [4], as shown using the peak field $\hat{B}_c = B_{c0} \cdot A_c$ substituting c with the x and z components.

$$P1 = \frac{S1}{S0} = \frac{\hat{B}_z^2-\hat{B}_x^2}{\hat{B}_z^2+\hat{B}_x^2}$$

$$P2 = \frac{S2}{S0} = \frac{2\hat{B}_x\hat{B}_z\mathrm{Cos}\,\delta}{\hat{B}_z^2+\hat{B}_x^2}$$

$$P3 = \frac{S3}{S0} = \frac{2\hat{B}_x\hat{B}_z\mathrm{Sin}\,\delta}{\hat{B}_z^2+\hat{B}_x^2}$$

These can be simplified by substituting the terms for phase shift (δ_c) and amplitude (A_c) to get Eq. (4).

$$P1 = \frac{\hat{B}_z^2-\hat{B}_x^2}{\hat{B}_z^2+\hat{B}_x^2}$$

$$P2 = \frac{\pm 2B_{x0}B_{z0}\mathrm{Sin}^2[k\phi_L]}{\hat{B}_z^2+\hat{B}_x^2} \quad (4)$$

$$P3 = \frac{B_{x0}B_{z0}\mathrm{Cos}[k\phi_L]\mathrm{Sin}[k\phi_E]}{\hat{B}_z^2+\hat{B}_x^2}$$

The nominal field components B_{xo} and B_{zo} are gap dependent terms which can be defined using an empirical function for the magnetic field versus gap, see Eq. (5).

$$B_{c0} = m\cdot e^{b1\left(\frac{g}{\lambda}\right)+b2\left(\frac{g}{\lambda}\right)^2+\cdots bn\left(\frac{g}{\lambda}\right)^n} \quad (5)$$

Typically for pure permanent magnet devices, B_{co}, uses only the first term b1. The coefficients of Eq. (5) can be determined using derived equations for an undulator field, or fitting to numerical magnetic models or magnetic measurements. In this analysis SRW [5] was used to compute the flux through a relevant opening aperture on the beamline using finite electron beam parameters for the CLS. The photon energy of the first harmonic peak was found

ISBN: 978-3-95450-208-0 doi:10.18429/JACoW-IPAC2019-TUPRB005

for multiple gaps in both horizontal and vertical polarisation modes. The coefficients for the nominal field components can be found using Eq. (6) as a fitting function for photon energy versus gap. B_{zo} can be determined from a horizontal polarisation mode when $A_x = 0$ and $A_z = 1$ and B_{xo} can be found from a vertical polarisation mode when $A_x = 1$ and $A_z = 0$. The best fit was attained using n = 2 for the periodic APPLE-II devices and n = 3 for the quasiperiodic devices. The higher order terms in the B_{co} fit help account for additional effects including the electron beam size and energy spread, a finite acceptance window, and a shift in the spectrum for the quasiperiodic device. The nominal field functions (B_{co}) could also be obtained from fits of photon energy versus ID gap measured at the beamline.

$$E_\gamma = \frac{2hc\gamma^2}{\lambda}\,\frac{1}{1+\frac{(0.0934\lambda)^2\left(A_x{}^2 B_{x0}{}^2 + A_z{}^2 B_{z0}{}^2\right)}{2}} \tag{6}$$

ARBITRARY POLARISATION

The polarisation rate and photon energy at any ID position can be determined using Eq. (4) and Eq. (6). The polarisation rates (P1, P2, P3) and photon energy (Eγ) represent three unknowns (since $P1^2 + P2^2 + P3^2 = 1$) defined using three independent variables (g, ϕ_E, ϕ_L). We can solve for the inverse numerically to find the ID position for any arbitrary polarisation. Combined with simulations of the beamline optics or polarimeter measurements taken on the beamline this will allow the calculation of the needed ID position to generate an arbitrary polarisation from the ID source which results in a desired polarisation at the sample (ex. P3= ±1) for a given photon energy.

RESULTS

Three APPLE-II devices have recently been constructed with magnetic periods of 55 mm, 142 mm and 180 mm, the latter being a quasiperiodic device. Magnetic measurements are taken at multiple ID positions and the measured fields can be used to simulate the expected photon flux at a beamline aperture using SRW. The photon energy at the first harmonic and the polarisation rates can also be calculated. These simulated results can be compared with values obtained from Eq (4) and Eq. (6).

The photon energies at multiple gaps are shown in Fig. 1, for each EPU at horizontal, vertical, and circular polarisations. Circle markers show the value of the first harmonic peak calculated using the measured magnetic field and SRW simulations of the EPU radiation. Cross markers show the value calculated using Eq. (6), with appropriate parameters for each device. Modelled photon energy has the best agreement with simulated results. Polarisation rates have better agreement where one stokes parameters equals 1. Photon energy as a function of elliptical phase is shown in Fig. 2, left and right chirality for circular polarisation and varying elliptical phase (ϕ_E) at fixed gaps and zero linear phase ($\phi_L = 0$) are shown for all three EPUs.

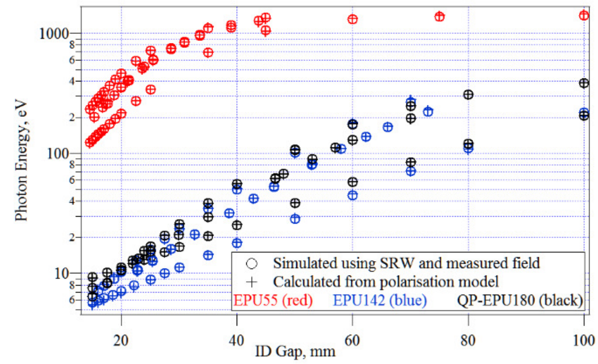

Figure 1: Horizontal, vertical, and circular polarisations are shown for each device as a function of gap.

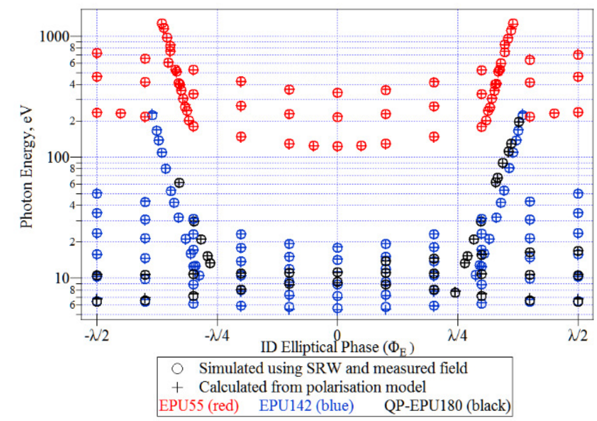

Figure 2: Circular polarisations and varying ϕ_E at fixed gap and $\phi_L = 0$ are shown for each device as a function of ϕ_E.

The polarisation rates can also be calculated using both the simulated results and values from Eq. (4). Comparisons for selected modes are shown for the P1 parameter versus ϕ_L and for P3 versus ϕ_E. Polarisation rates are shown for all three EPUs in Fig. 3 and Fig. 4. In each figure either ϕ_E or ϕ_L respectively is fixed at zero and the gap is fixed at the minimum set point, 15 mm for EPU142 and QP-EPU180 or 14.5 mm for EPU55.

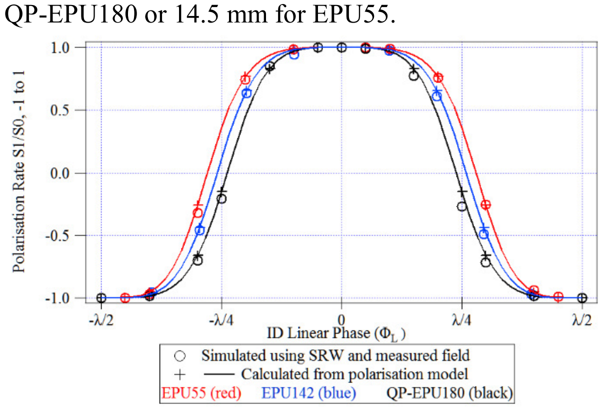

Figure 3: Polarisation rates P1 versus ϕ_L at fixed gap and $\phi_E = 0$.

The solid line shows the continuous variation of polarisation rate as calculated from the polarisation model. The

ISBN: 978-3-95450-208-0 doi:10.18429/JACoW-IPAC2019-TUPRB005

crosses show the discrete values of the model using the exact ID positions corresponding to the measured field used in the SRW-simulated value (circles).

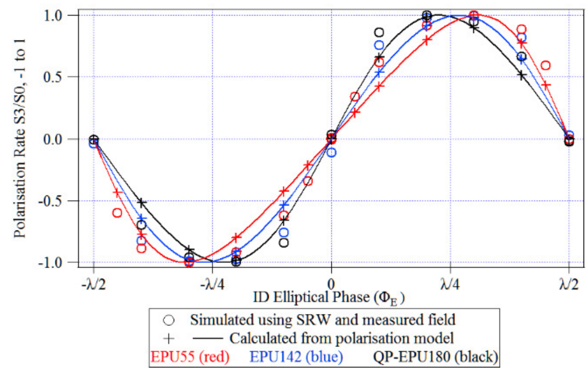

Figure 4: Polarisation rates P3 versus ϕ_E at fixed gap and $\phi_L = 0$.

Extensive measurements were made of EPU142 in universal polarisation modes when both ϕ_E and ϕ_L are nonzero. The results of 54 magnetic field measurements at a 15mm gap are shown in Fig. 5 to 8 for three cases of universal mode when: $\phi_E = \pm 2 \cdot \phi_L$; $\phi_E = X$, $\phi_L = \pm\lambda/8$; or $\phi_E = X$, $\phi_L = \pm\lambda/4$.

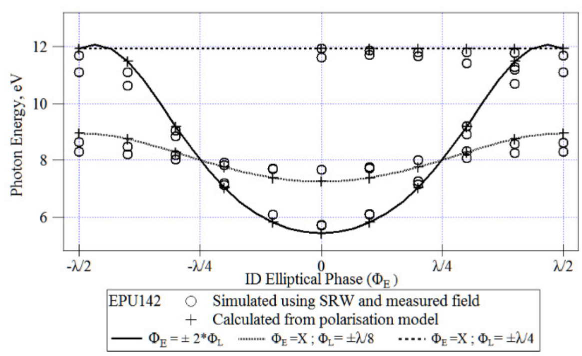

Figure 5: Photon energies for EPU142 in universal polarisation modes.

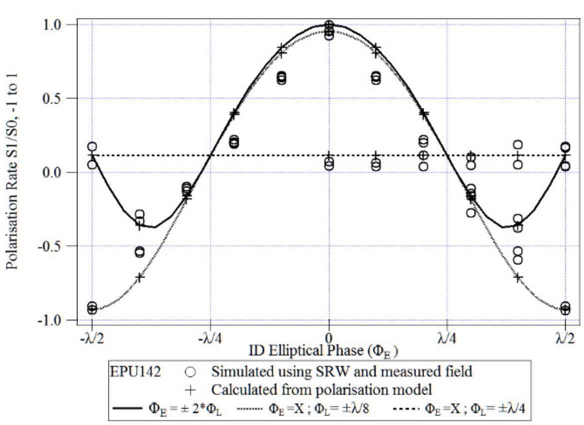

Figure 6: Polarisation rate P1 for EPU142 in universal polarisation modes.

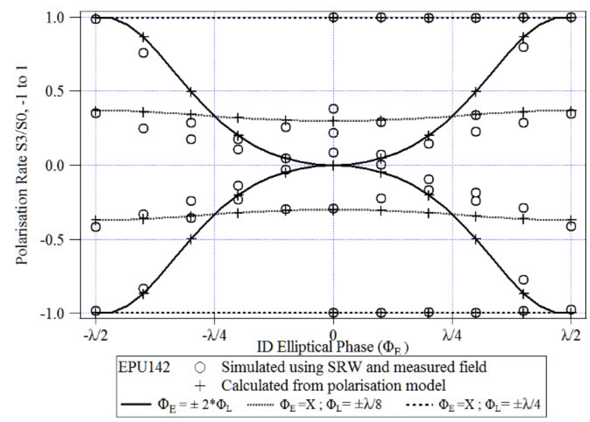

Figure 7: Polarisation rate P2 for EPU142 in universal polarisation modes.

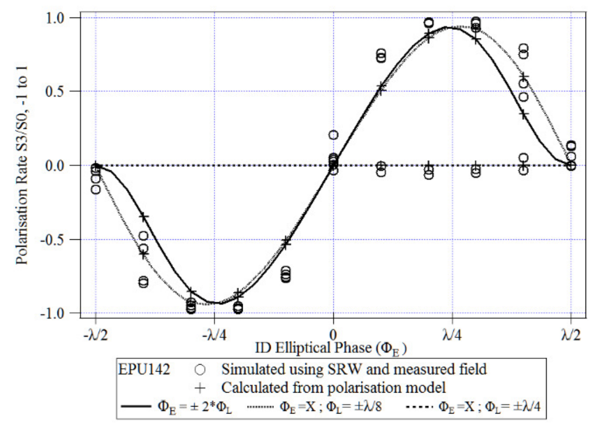

Figure 8: Polarisation rate P3 for EPU142 in universal polarisation modes.

CONCLUSION

The polarisation rate and photon energy at the first harmonic peak can be determined for any arbitrary girder position of an APPLE-II type EPU in universal polarisation mode. Improvements to fitting parameters may be obtained by using spectrum measurements taken by the beamline from a limited number of gaps in horizontal and vertical polarisations. Simulations of beamline optics can be used to calculate the required polarisation from the ID source to get pure circular polarisation at the beamline sample position. Numerical solutions of these equations can also be solved for the inverse problem to determine the ID set point needed for any required polarisation.

REFERENCES

[1] C. K. Baribeau, L. O. Dallin, J. M. Helfrich, T. M. Pedersen, M. J. Sigrist, and W. A. Wurtz, “Simulated and measured magnetic performance of a double APPLE-II undulator at the Canadian Light Source”, in *Proc. IPAC'16*, Busan, Korea, May 2016, pp. 4025-4027.

[2] C. K. Baribeau, T. M. Pedersen, M. J. Sigrist, and W. A. Wurtz, “Virtual shimming and magnetic measurements of two long period APPLE-II undulators at the Canadian Light Source”, presented at IPAC'19, Melbourne, Australia, May 2019, paper TUPRB003, this conference.

ISBN: 978-3-95450-208-0 doi:10.18429/JACoW-IPAC2019-TUPRB005

[3] T. Schmidt and D. Zimoch, "About APPLE II operation", *AIP Conference Proceedings*, Vol 879:1, pp 404-407, 2007.

[4] J. A. Clarke, "Generation of polarized light", in *The Science and Technology of Undulators and Wigglers*, New York, NY, USA: Oxford University Press, 2004, pp. 99-101.

[5] O. Chubar and P. Elleaume, "Accurate and efficient computation of synchrotron radiation in the near field region", in *Proc. EPAC'98*, Stockholm, Sweden, Jun. 1998, paper THP01G, pp. 1177-1179.